AMERICAN SOCIETY FOR MICROBIOLOGY | Applied and Environmental Microbiology

| Bacteriophages | Full-Length Text

Viral enumeration using cost-effective wet-mount epifluorescence microscopy for aquatic ecosystems and modern microbialites

Madeline Bellanger,[1,2] Pieter Visscher,[3] Richard Allen White III[1,2]

AUTHOR AFFILIATIONS See affiliation list on p. 10.

ABSTRACT Enumeration is a fundamental measure of community ecology in which viruses represent the most numerous biological identities. Epifluorescence microscopy (EFM) has been the gold standard method for environmental viral enumeration for over 25 years. Currently, standard EFM methods using the Anodisc filters are no longer cost-effective (>$15 per slide) and have yet to be applied to modern microbialites. Microbialites are microbially driven benthic organosedimentary deposits that have been present for most of Earth's history. We present a cost-effective method for environmental viral enumeration from aquatic samples, microbial mats, and exopolymeric substances (EPSs) within modern microbialites using EFM. Our integrated approach, which includes filtration, differential centrifugation, chloroform treatment, glutaraldehyde fixation, benzonase nuclease treatment, probe sonication (EPS and mat only), SYBR Gold staining, wet mounting, and imaging, provides a robust method for modern microbialites and aquatic samples. Viral abundances of modern microbialites and aquatic samples collected from Fayetteville Green Lake (FGL) and Great Salt Lake (GSL) did not differ across ecosystems by sample type. EPS and microbial mat samples had an order of magnitude higher viral-like particle abundance when compared to water regardless of the ecosystem (10^7 vs 10^6). Viral enumeration allows for estimates of total viral numbers and weights. The entire weight of all the viruses in FGL and GSL are ~598 g and ~2.2 kg, respectively. Further development of EFM methods and software is needed for viral enumeration. Our method provides a robust and cost-effective (~$0.75 per sample) viral enumeration within modern microbialites and aquatic ecosystems.

IMPORTANCE Low-cost and robust viral enumeration is a critical first step toward understanding the global virome. Our method is a deep drive integration providing a window into viral dark matter within aquatic ecosystems. We enumerated the viruses within Green Lake and Great Salt Lake microbialites, EPS, and water column. The entire weight of all the viruses in Green Lake and Great Salt Lake are ~598 g and ~2.2 kg, respectively.

KEYWORDS viruses, bacteriophage (phage), epifluorescence microscopy, stromatolites, thrombolites, microbialites, Fayetteville Green Lakes, NY, Great Salt Lake, UT

Viruses are the most numerous "biological entity" on Earth, with a ubiquitous range across every environment and an estimated global abundance of 10^{31} viral-like particles (VLPs) (1–4). This 10^{31} VLP estimate (i.e., Hendrix product) accounts mainly for double-stranded DNA phage abundances (2–4). This estimation did not include the diversity of large DNA, RNA, and ssDNA viruses (4). Viral abundance estimates may be an underestimation as 10^{30} viruses are estimated to exist in the ocean alone (5), and global

Editor John R. Spear, Colorado School of Mines, Golden, Colorado, USA

Address correspondence to Richard Allen White, rwhit101@charlotte.edu.

The authors declare no conflict of interest.

See the funding table on p. 10.

Received 3 October 2023
Accepted 12 October 2023
Published 28 November 2023

biomass estimates (6) suggest more measurements and method developments are still needed.

Epifluorescence microscopy (EFM) is the gold standard technique for the enumeration of microbes and viruses (7), which includes the enumeration of aquatic bacteria since 1977 (8), but its use for viruses began in the early 1990s (9). Viruses play critical roles in the life and death cycles of microbes through viral lysis that interplays in global biogeochemical cycles (e.g., carbon and nitrogen pool), population dynamics, marine viral shunt, and nutrient transportation (5, 10–16). Aquatic systems remain the most enumerated ecosystems for viruses, with soils and sediments being a close second, and microbial mats rarely, followed by none for modern microbialites. Enumeration is the first critical step in understanding an ecosystem; thus, viral enumeration represents a major factor in microbial community ecology.

Microbial mats are laminated organosedimentary ecosystems that can form microbialite carbonate structures through mineral precipitation [i.e., lithification (17–19)]. Microbialites are benthic microbial deposits (20) that accrete as a result of a microbial community trapping and binding sediments and forming the locus of mineral precipitation (17–19). Not all microbial mats can become microbialites; this depends on both abiotic (e.g., water hardness and cation concentration) and biotic (e.g., microbial metabolic activity) factors (21). Microbialites have been present for 80% of geological history (e.g., 3.7 Gyr) and provide a modern proxy for ancient ecosystem formation (21, 22). Precipitation of carbonates is facilitated by cyanobacterial photosynthetic alkalization and filament trapping/binding using exopolymeric substances (EPSs) (17–19). EPS is primarily produced by cyanobacteria and some heterotrophic bacteria within mats and trap sediments, allowing for the stabilization and accretion of carbonates (17–19). EPS density, pH, and carbohydrate structure act as the site of mineral nucleation by binding cations that can influence mineral morphologies and carbonate precipitation (23, 24). EPS has also been shown to bind viruses and microbes within microbial mats (25). Viruses, particularly cyanophages, have been proposed as the missing mechanism for understanding how soft microbial mats transition to hard carbonate microbialites (26). Virus–host interactions may support the formation of microbialites through the alteration of microbial metabolism (specifically photosynthesis), the development of viral resistance strategies, or gene alteration impacting EPS production (26).

EFM and flow cytometry (FCM) are the most widely utilized methods for enumerating VLPs (7, 27, 28). Classically, viral enumeration was measured by transmission electron microscopy (TEM) (7, 29, 30). TEM approaches for viral enumeration were problematic for routine use due to being labor-intensive, having large specimen variability, and being expensive (7, 29, 30). EFM was more accurate and precise in measuring viruses than TEM (29). Current EFM viral enumeration methods require expensive Whatman Anodisc filter 0.02 µm (catalog number WHA68096002) membranes (i.e., $16.32 per filter). These filters are required for EFM enumeration for viruses. However, they are only produced by a single manufacturer and have had shifts in supply and price increases via global inflation due to the COVID-19 pandemic. The filters have been over US $10 for over a decade with no sign of price reduction. A more cost-effective method is needed to scale global sampling enumeration for viruses.

EFM viral enumeration has been previously applied to microbial mats but not microbialites (25). Carreira et al. (25) tested a variety of buffers (e.g., tetrasodium pyrophosphate vs EDTA), nucleases (e.g., DNase I/RNase I vs benzonase), and sonication methods (e.g., bath vs probe) (25). The Carreira et al. (25) method suggested optimal EFM conditions for microbial mats: glutaraldehyde fixation (i.e., 2%), 0.1 mM EDTA, and benzonase treatment with probe sonication (25). However, this method requires Anodisc membrane filters, which makes it no longer cost-effective.

Wet-mount EFM has been suggested as a cost-effective alternative to Whatman Anodisc filter membrane-based protocols (31). This EFM method relies on chemical flocculation concentration of the VLPs using iron chloride precipitation, followed by EDTA–ascorbate resuspension, SYBR Gold nucleic acid staining, and wet mounting on a

standard glass slide (31). With and without chemical flocculation-based wet mount, EFM showed similar concordance and precision with Anodisc-based methods at a much lower cost (31). It also was effective for natural ambient marine and freshwater ecosystems from the low end of 1×10^6 mL^{-1} to a high end of 1×10^8 mL^{-1}, similar to Anodisc methods (31). The wet-mount method has yet to be applied for solid non-aquatic samples such as soils, microbial mats, sediments, or microbialites.

There has been an ongoing debate about whether membrane-derived vesicles (MDVs), free extracellular DNA (FED), gene transfer agents, and cell debris may produce "fake particles" that are labeled as VLPs (32). They suggested improving EFM and FCM for viral enumeration by adding a chloroform step to limit MDVs and cellular debris and a nuclease step to remove FED (32). Ribosomes with rRNAs could also be co-purified in viral preparations, which could be mistaken for viruses if clumped together but are reduced by chloroform treatment (33). Membrane-bound viruses are sensitive to chloroform and some phage (e.g., *Corticoviridae* and *Inoviridae*) (32). Viruses can be resistant to nuclease treatment, including RNA phages (e.g., MS2) (25, 34)

Here, we present a cost-effective method of EFM to enumerate viruses in aquatic environments, microbial mats, EPS within microbial mats, and modern microbialites within the Great Salt Lake (GSL) and Fayetteville Green Lake (FGL). Our method incorporates wet mounting (31), Carreira et al. (25), and the suggestions of Forterre et al. (32) to have a uniform method of EFM across aquatic ecosystems, microbial mats, and microbialites (25, 32). The enumeration of viruses within modern microbialites could illuminate the microbial–viral–mineral interactions and mechanisms required to transition from soft microbial mat to hard carbonate lithified microbialite.

MATERIALS AND METHODS

Sample collection

Water and microbialite samples were collected in Great Salt Lake (Antelope Island State Park, Utah, 41°N, 112°W, GSL, near Layton, UT) and Green Lake (Green Lake State Park, New York, 43.049°N, 75.973°W, FGL, near Fayetteville, New York).

Preparation of nucleic acid stain working stock

The working stock was created from a commercial stock of SYBR Gold (Invitrogen, S11494), thawed in the dark at room temperature. Once thawed, the commercial stock was vortexed for 10 s at medium-high speed (1,000 RPM), then centrifuged at 2,000 relative centrifugal fields (RCFs) in a microcentrifuge for 5 min. The commercial stock was then diluted 1:10 with autoclaved and filtered (0.22 µm PVDF Millipore, GVWP06225) molecular biology-grade water. The working stock was filtered (0.22 µm PVDF filters) before small volumes (~300 µL) were aliquoted into microcentrifuge tubes wrapped in aluminum foil or black microcentrifuge tubes and stored at −20°C until use.

Preparation of samples

Samples were prepared similarly across the water, whole microbial mat, and EPS, which included filtration, differential centrifugation, chloroform treatment, glutaraldehyde fixation, benzonase nuclease treatment, probe sonication (EPS and mat only), SYBR Gold staining, wet mounting, and imaging (Fig. 1). Water samples from GSL and FGL were prepared with an optional concentration step using 30 kDa MWCO pore-size centrifugal filter devices (Millipore, UFC5030). Water samples (i.e., 500 mL) were filtered twice through 0.22 µm PVDF filters and then concentrated in Centricon-70 plus centrifuge filters (Millipore, UFC703008, 30 kDa) in 12 min increments at 3,000 RCF. Flow through water (i.e., ultrafiltrate) was collected after each centrifugation step. A final centrifugation step of 5 min at 1,000 RCF was used to collect the filtrate by flipping the filter into the collection cup to obtain a concentrated viral sample. Viral concentrated water was

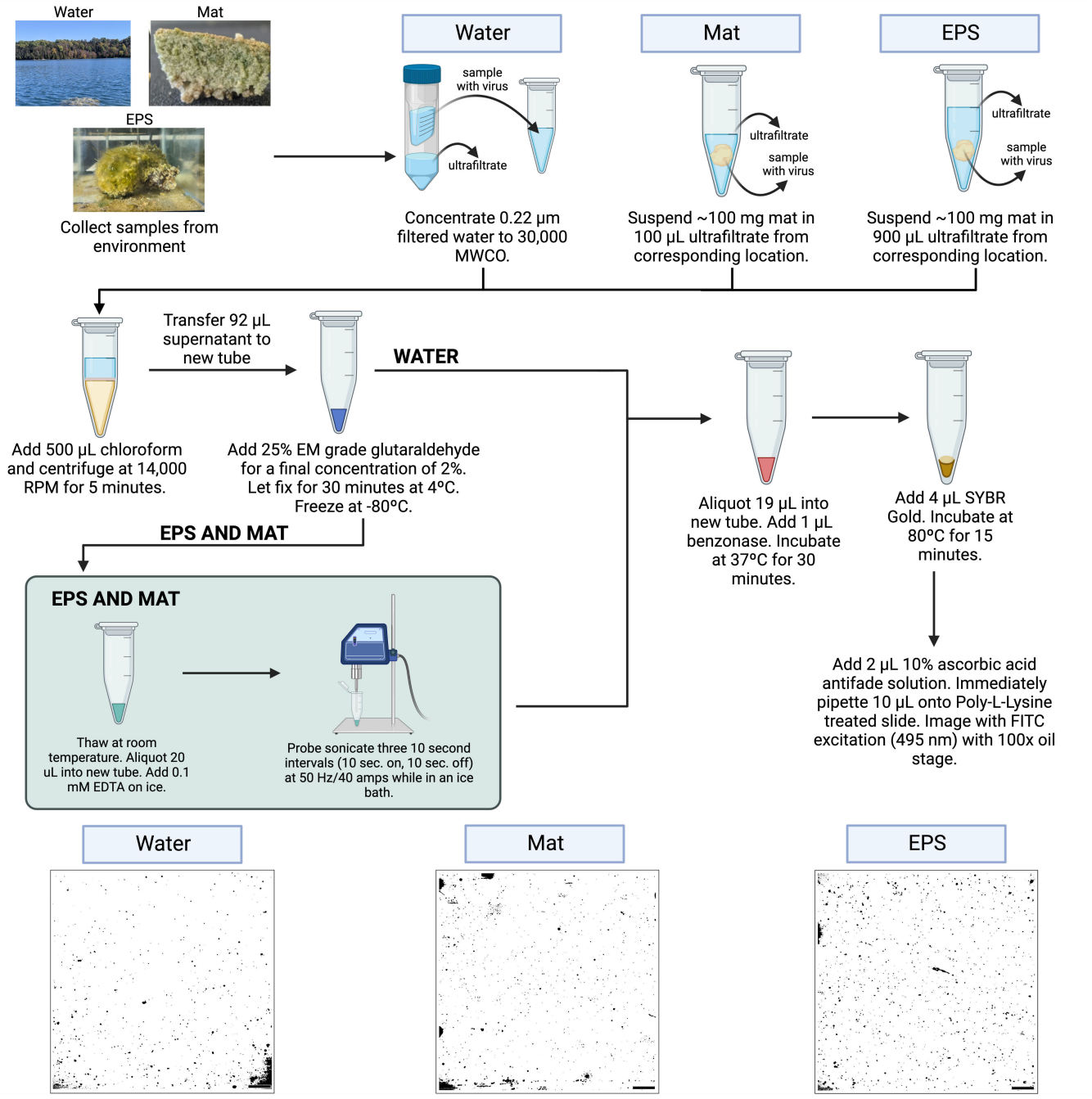

FIG 1 Flow diagram of EFM protocol. This diagram provides a detailed methodological walk-through of the preparation of water, microbial mat, and EPS samples.

recovered from Centricon-70, then diluted to 1 mL with ultrafiltrate from the original location.

Whole microbial mats and EPS were resuspended in matching location ultrafiltered water (i.e., 30 kDa filtered). Approximately 100 mg of the microbial mat was taken for the whole mat vs EPS samples. The whole mat was resuspended in 100 µL of ultrafiltrate vs 900 µL of ultrafiltrate for EPS (Fig. 1). All samples were treated with 500 µL of chloroform, then differential centrifugation, fixation with glutaraldehyde (2% final concentration), benzonase treatment, staining with SYBR Gold, and then wet mounting (Fig. 1). EPS and mat samples required additional treatments to get rid of cell debris, FED, and

MDVs. Before benzonase treatment, EDTA was added to EPS and the whole mat for a final concentration of 0.1 mM, as suggested by Carriera et al. (25). Then, samples were probe sonicated, and the supernatant was transferred to a new tube prior to nuclease treatment by benzonase (Fig. 1). For all samples, benzonase treatment included 19 µL of sample with 1 µL benzonase (25 U) added, then incubated in a heat block at 37°C for 30 min (Fig. 1). Samples were frozen and then stored at −80°C until use.

Preparation of wet mounting, slide preparation, and microscopy

Slides were prepared before thawing samples by thoroughly cleaning them with 70% ethanol. After cleaning, the slides were allowed to dry before soaking in a 10% poly-L-lysine solution in a polystyrene dish for 5 min. After soaking, the slides were drained and dried in a drying oven at 60°C for 1 hour. The slides were then removed from the oven and stored in a microscope slide box until use.

SYBR Gold stock was aliquoted in the dark to avoid stain decay; then, 4 µL of SYBR Gold working stock was added to each sample and pipetted to mix. The tubes were then incubated at 80°C in a heat block for 15 min in the dark. After incubation, samples were removed from the heat block and mixed with 2 µL of freshly prepared ascorbic acid antifade solution (10% ascorbic acid wt/vol in 1× PBS and filtered through 0.22 µm PVDF filters twice) (31); 10 µL of each sample was immediately pipetted onto poly-L-lysine-treated slides, covered with a cover slide, and imaged on an Olympus IX83 microscope under FITC blue excitation light (495 nm) with a 100× oil stage (Fig. 1).

Enumeration

VLPs were counted in EFM images according to size and shape. Particles were included if they were <300 nm, which can be trained through images of beads of known sizes (175 ± 5 nm) (Fig. S4). These fluorescent beads from Molecular Probes' PS-Speck Microscope Point Source Kit (P7220) with excitation and emission wavelengths of 360 nm/440 nm were added to each slide at 100× dilution (~3.5 µL per slide) for training purposes. Large particles, halo autofluorescence, and clumps of VLPs were excluded from counting. At least three slides with at least three images per slide and a minimum of 12 images total were averaged for each by location and sample type (e.g., GSL mat) (Fig. S3). Automatic counts from programs such as ImageJ provided inaccurate results. Due to this, all images were manually counted and corrected by eye. Images with fewer than 100 VLPs and more than 500 VLPs were excluded. Exposure and contrast were adjusted to increase countability, and images were converted to negatives to increase the visibility of small particles. The field of view was calculated by finding the image's area in micrometer using the length and width found with the Olympus cellSens software. Cover slides of 22 × 22 mm were used. The area of the cover slides was calculated by multiplying the length by the width and was converted to micrometer. The scaling factor was calculated by dividing the cover glass area by the field of view. This value was then used to multiply the counts for each image to determine the number of viral particles in 10 µL used per slide. Water samples were adjusted to account for concentration and then converted to determine VLPs mL^{-1}. VLP concentrations for microbial mat and EPS samples were calculated by multiplying the counts by the same scaling factor as with water samples, dividing by 10 µL, multiplying by the dilution factor, and then dividing by the mass of microbial mat or EPS sample used (~0.10 g).

Statistical analysis

All statistical analyses were performed with R. A total of 150 images were analyzed across all sample types. A test of normality was first done for each sample type using the Shapiro–Wilks test (Table S1). Eleven sample types were tested. If both samples were normally distributed, an *F*-test was conducted to test for equal variances. A total of 10 sample comparisons were tested for equal variances. Thirteen sample comparisons were made with Student's *t*-test, Wilcoxon rank sum test, and Welch's *t*-test, depending on sample conditions (Table S2).

RESULTS

VLPs across sample types varied but not across ecosystems (FGL vs GSL). GSL and FGL had similar viral abundances at ~1 × 10^6 VLPs mL^{-1} (i.e., 1.43 × 10^6 mL^{-1} GSL vs 9.95 × 10^5 VLPs mL^{-1} FGL, Fig. 2). GSL VLPs appeared to have smaller and more uniform sizes than FGL (Fig. 2). The coefficient of variance (CV) was higher in FGL than in GSL (38.79% FGL vs 19.15% GSL). Large particles were present in FGL water that were >300 nm and lacked uniform VLP size. EPS had the highest VLP counts observed. EPS had an order of

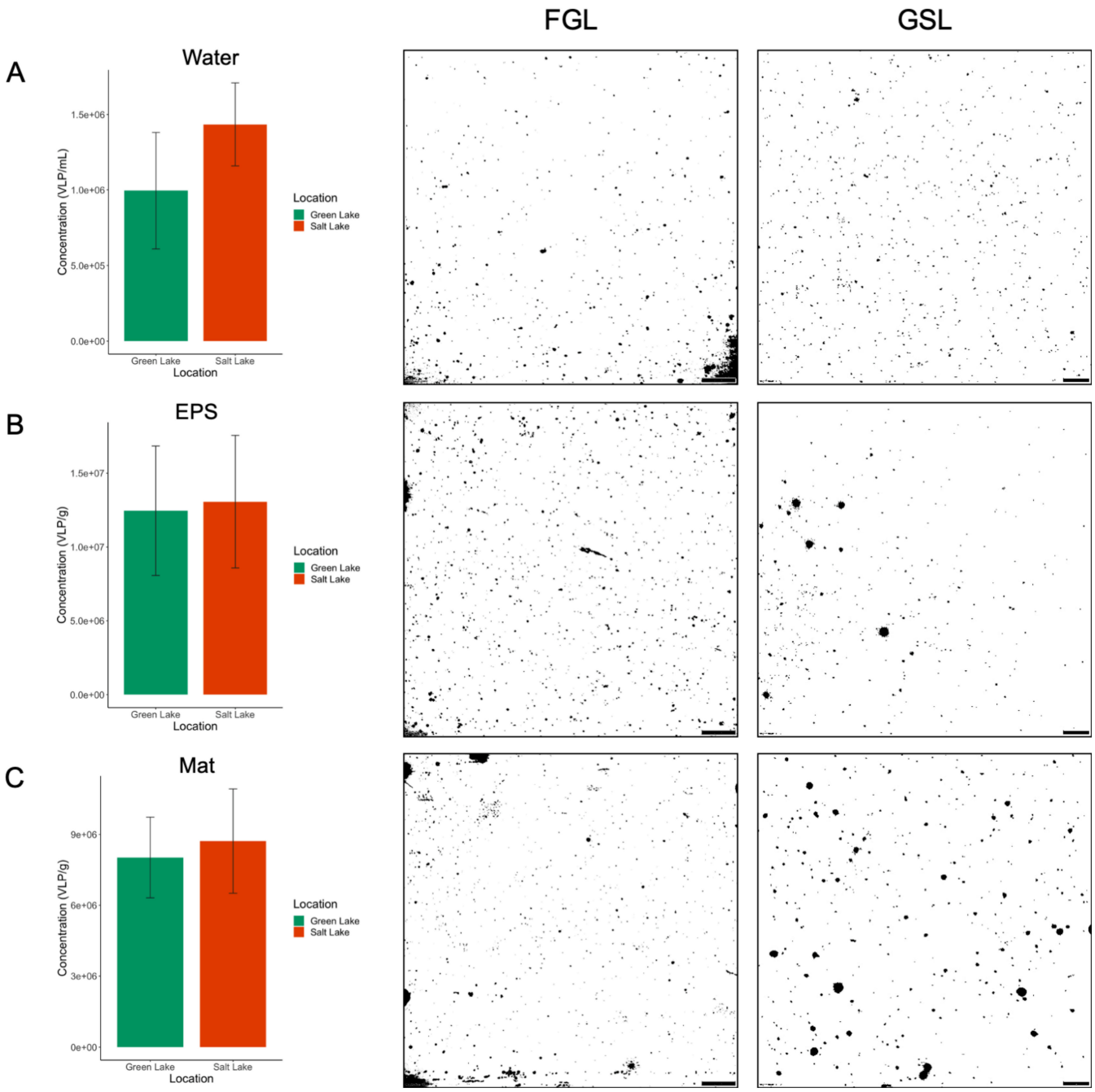

FIG 2 Viral enumeration of GSL and FGL. EPS and whole mat VLPs are expressed as g^{-1} vs mL^{-1} for water samples. All images are under 100× oil immersion with a scale bar equal to 200 pixels or 10 µm. All images were converted to negatives to increase the visibility of VLPs. (A) Average VLP concentrations for water samples with representative EFM images. (B) Average VLP concentrations for EPS samples with representative EFM images. (C) Average VLP concentrations for mat samples with representative EFM images.

magnitude higher abundance of VLPs than water with ~1 × 10^7 VLPs g^{-1} (i.e., 1.25 × 10^7 g^{-1} FGL vs 1.31 × 10^7 VLPs g^{-1} GSL) with similar CVs (35.26% FGL vs 34.40% GSL, Fig. 2). Whole mat samples had higher VLPs than water as well as with 8–9 × 10^6 g^{-1} (i.e., 8.02 × 10^6 g^{-1} FGL vs 8.72 × 10^6 VLPs g^{-1} GSL) with similar CVs (21.32% FGL vs 25.33% GSL, Fig. 2). GSL and FGL did not differ statistically across ecosystems within the sample type (e.g., EPS FGL vs GSL) and had similar viral abundances (Table S2). Low (<4.0 × 10^5 VLPs mL^{-1}) and high (>2.0 × 10^7 VLPs mL^{-1}) samples are well within our detection limits using this method.

Our protocol added a chloroform step to all samples and a benzonase treatment to aquatic samples. The chloroform and benzonase treatment did remove large cellular debris, MDVs, and FED (Fig. S5 to S7). We confirm the results from Carriera et al. (25) that probe sonication is superior to water bath-based and EDTA was better than tetrasodium pyrophosphate and that benzonase treatment cleared FED better than DNase I only or DNase/RNase (Fig. S5 to S7). Chloroform offered greater removal of cellular debris of aggregated VLPs or MDVs in carbonate-rich EPS and mat from microbialites than without (Fig. S5 to S7).

The Cunningham method requires chemical flocculation concentration of the VLPs using iron chloride precipitation, followed by EDTA–ascorbate resuspension for preparing samples (31). We tested this on our aquatic samples and had similar results but found that chloroform and benzonase treatment cleared the images providing better quality. We found high concordance in aquatic samples with and without chemical flocculation. Thus, we opted out of using it due to the extra steps required. Chemical flocculation did not work for EPS or mat from modern microbialites in our hands. We were unable to resuspend samples post-flocculation.

Poly-L-lysine was another addition to our protocol over others that provided an added benefit. The addition decreased CVs across images, allowed for more precise placement of VLPs across the slide, made the field of view of VLPs more uniform, and provided greater storage stability of VLPs on slides. Slides made even a month later had <1% drop in viral counts using poly-L-lysine (Fig. S1).

Cost analysis suggests that Anodisc filter-based methods are >$15 a sample (Table 1). The Cunningham method is currently the most cost-effective method, originally costing ~$0.10 per sample in 2015, but the original beads used in their study are no longer in manufacture (Table 1) (31). We used a similar-sized bead that is available for our cost estimation (2.06-µm bead), which, due to inflation, now makes the method cost almost double in less than a decade (~$0.18 per sample) (Table 1). We recommend benzonase and chloroform treatment with the standard Cunnigham method; the price increases to ~$0.84 per sample, but both will improve image quality (Table 1) (31). Our method is ~$0.75 per sample, mainly due to the cost of benzonase, which is more expensive than DNase I/RNase I combined but is superior (Table 1).

TABLE 1 Cost analysis of EFM approaches[a] for counting bacteria and viruses in water, microbial mats, and EPS[b]

Method	Cost (USD)
Bellanger et al. presented here	$0.75
Cunningham et al. (31) (water)	$0.18[c]
Advanced Cunningham (water)	$0.84[d]
Carreira et al. (25) (mat)	$18.79
Budinoff et al. 2011 (water)	$22.12
Noble and Fuhrman (7), (water)	$16.18

[a]Values calculated during the COVID-19 pandemic and inflation period of 2022 have caused costs and supply fluctuations.
[b]The cost of consumables (pipette tips, microcentrifuge tubes, etc.) is estimated to be the same for each method.
[c]Original bead size (2.34 µm) is no longer in manufacture. A similar-sized bead (2.06 µm) was used to calculate cost instead.
[d]Advanced method is the Cunningham method with added chloroform and benzonase.

DISCUSSION

Our EFM protocol is an integration of multiple methods in order to provide results across both aquatic and solid substrate ecosystems (25, 31, 32). These integrations are used to analyze VLPs over fake particles (32). Our study confirms suggestions that chloroform and nuclease treatment clears images and removes FEDs, MVDs, and cellular debris. Furthermore, it confirms the results of Carriera et al. (25) with some additions that can be applied to microbial mats and EPS on solid carbonate microbialites, including a wet-mount method that removes the expensive Anodisc filter requirement (25). We could not use chemical flocculation on microbial mats and EPS from modern microbialites with any success. Further method development is needed to use chemical flocculation within microbial mats and EPS in modern microbialites or other solid substrate ecosystems such as soils or sediments.

FGL and GSL had relatively the same VLP concentrations regardless of the sample type and did not differ statistically. EPS had the highest VLP concentration at ~10^7 g^{-1}. However, the whole microbial mat also had similar abundances 8–9 × 10^6 g^{-1}, which was an order of magnitude higher than surrounding water suggesting VLPs are being trapped or concentrated within the mat and/or EPS. Observation of whole microbial mats shows VLPs trapped on the surface layers, which has been suggested previously (25, 35), which we confirm here. These viruses may act as nucleation sites for carbonate minerals within the microbialite mat (35, 36).

Previously, soft intertidal marine microbial mats (i.e., not hard carbonate microbialites) in Schiermonnikoog Island, the Netherlands, had some of the highest measured VLPs ever recorded at 2.8 × 10^{10} g^{-1} (25). We find that GSL and FGL microbialite mats do not have these similar high abundances as intertidal marine microbial mats. They are more similar to standard aquatic VLP abundances within freshwater samples ~10^6–10^7. EPSs within GSL and FGL microbialites are in the low range of VLP abundance in soils which ranges from 10^7 to 10^9 (37). Our microbialites are present in meromictic lakes that do not seasonally turnover or mix beyond rainfall, suggesting less bacterial mixing, whereas intertidal zones have continuous mixing and influx of microbes, including virally infected microbes. Previous metagenomic analysis of both Pavilion Lake and Shark Bay microbialites and microbial mats found viruses present, but high gene abundance of viral defense clusters (38–40). Pavilion Lake metagenomes had statistically higher viral genes present in microbialite surrounding water metagenomes than microbialite metagenomes (38).

Viral counting is done manually by eye for all current EFM methods. While software such as ImageJ exists, it struggles with automatic counts within images with large particles, halo autofluorescence, and clumps of VLPs. ImageJ was unable to count VLPs accurately across our samples in general. While counting manually is very labor-intensive and requires training for accurate VLP counting, it is our only current option. Manual counting may miss dim low fluorescence containing VLPs, small VLPs, and VLPs underneath halo autofluorescence, and general human error can occur, but it is limited by proper training. Future software and algorithm development is needed to alleviate the labor-intensive nature of manual VLP counting for EFM.

Currently, our method enumerates viruses regardless of the nucleic acid type and strandedness and accounts for the large viruses. Further improvements are needed in EFM dyes to distinguish single-stranded vs double-stranded nucleic acids when mixed. Also, giant viruses, including pandoraviruses, are commonly filtered out during standard filtration of 0.22 µm (41). Acridine orange may be selective for RNA over DNA in fluorescence shift and effective for ssDNA phages (42, 43). Chloroform without filtration has been useful in removing bacteria to isolate jumbo and megaphages (44). Antibiotics and fungicides may be useful for membrane-bound giant viruses like pandoraviruses to remove bacteria and fungi in enumeration studies (41). DAPI and Yo-Pro-I were used for viral enumeration but were too dim compared to SYBR-based options (30). SYBR Green I and SYBR Gold were equivalent for virus and bacterial enumeration (30). SYBR Green

I/II or SYBR Gold can be used for RNA virus staining (30), but not in RNA and DNA virus mixed samples.

Counts of viruses in EFM samples can broadly estimate the abundance of viruses within the water, microbial mats, and overall systems of FGL and GSL. The lake volumes can change for various environmental (i.e., seasonally and precipitation) and anthropogenic reasons. Similarly, viral concentrations may vary seasonally and spatially (with depth and relation to the shore) (45). With these understandings, approximations of viral abundance and total weight are derived from our measurements. The volume of FGL is estimated to be 7,235,900 m^3 (46). For FGL, based on the total volume, which is 7.2×10^{12} mL times the average VLP concentration of 9.95×10^5 mL^{-1}, the total number of viruses is 7.2×10^{18} VLPs. If we assume that each virus weighs at least 50×10^6 daltons (based on coliphage T7) (47) and convert daltons to grams using the Avogadro constant (1.66×10^{-24}), then the weight of all the viruses present within FGL is ~598 g. A standard loaf of bread weighs roughly 500 g. The volume of all FGL viruses, if concentrated all together, could fit in a standard salad dressing bottle. GSL is estimated to contain 11.42–18.92 km^3 (48). Converting km^3 into mL yields $1.1–1.9 \times 10^{16}$ mL total volume times the average VLP concentration of 1.43×10^6 mL^{-1}, resulting in ~2.7×10^{22} VLPs total in GSL. If we assume that the average weight is 50×10^6 daltons and convert daltons into kilograms using the Avogadro constant (1.66×10^{-27}), then the weight of all the viruses in GSL is ~2.2 kg. The mass of viruses in the GSL (i.e., ~2.2 kg) is equivalent to a standard-size red brick, which could fit within a gallon container.

Further advancements are needed to directly measure viruses to understand how many viruses are present within natural ecosystems beyond what is presented here. The development of EFM methods using various nucleic acid, protein, and lipid stains may help to distinguish between intact viral particles and expose their presence regardless of their nucleic acid type, strandedness, or size. Seasonal measures of the viral abundances are needed within GSL and FGL waters and microbialites to enumerate any variation, especially GSL, which has experienced record lows due to droughts. Enumeration is the first critical step in the ecology of an ecosystem. Our method is an advancement toward robust viral measurement within modern microbialites, microbial mats, and aquatic ecosystems that are cost-effective (~$0.75 per sample).

ACKNOWLEDGMENTS

We acknowledge the UNC Charlotte University Research Computing Community and the UNC Charlotte College of Computing and Informatics for computational and logistical support.

R.A. White III and Madeline Bellanger are supported by the UNC Charlotte Department Bioinformatics and Genomics start-up package from the North Carolina Research Campus in Kannapolis, NC, and by the National Aeronautics and Space Administration (NASA) Exobiology project NNH22ZDA001N-EXO. National Science Foundation (NSF) supports Pieter Visscher grant OCE 1561173 (USA) and ISITE project UB18016-BGS-IS (France).

Conceptualization was performed by R.A.W. III, M.A.B., and P.V.; methodology was performed by M.A.B. and R.A.W. III; investigation was performed by M.A.B. and R.A.W. III; writing (original draft) was performed by M.A.B. and R.A.W. III; writing (review and editing) was performed by R.A.W. III, M.A.B., and P.V.; funding acquisition was performed by R.A.W. III and P.V.; resources were secured by R.A.W. III and P.V.; supervision was performed by R.A.W. III.

The authors declare no conflicts of interest. R.A.W. III is the CEO of RAW Molecular Systems (RAW) LLC, but no financial support, IP, or others from RAW LLC were used or contributed to the study.

AUTHOR AFFILIATIONS

[1]Department of Bioinformatics and Genomics, North Carolina Research Campus, The University of North Carolina at Charlotte, Kannapolis, North Carolina, USA
[2]Computational Intelligence to Predict Health and Environmental Risks (CIPHER), The University of North Carolina at Charlotte, Charlotte, North Carolina, USA
[3]Department of Marine Sciences and Geoscience, University of Connecticut, Storrs, Connecticut, USA

AUTHOR ORCIDs

Madeline Bellanger http://orcid.org/0009-0007-2021-4697
Richard Allen White III http://orcid.org/0000-0002-6292-5936

FUNDING

Funder	Grant(s)	Author(s)
NASA | NASA Astrobiology Institute (NAI)	NNH22ZDA001N-EXO	Madeline Bellanger Pieter Visscher Richard Allen White III

AUTHOR CONTRIBUTIONS

Madeline Bellanger, Conceptualization, Data curation, Formal analysis, Investigation, Methodology, Software, Validation, Visualization, Writing – original draft, Writing – review and editing | Pieter Visscher, Conceptualization, Funding acquisition, Investigation, Project administration, Writing – original draft, Writing – review and editing | Richard Allen White III, Conceptualization, Data curation, Formal analysis, Funding acquisition, Investigation, Methodology, Project administration, Resources, Software, Supervision, Validation, Visualization, Writing – original draft, Writing – review and editing

DATA AVAILABILITY

Raw image files and supplemental data are all available at https://osf.io/f8be4/. All code and statistical calculations for this study are available on www.github.com/raw-lab/efm.

ADDITIONAL FILES

The following material is available online.

Supplemental Material

Supplemental file 1 (AEM01744-23-s0001.pdf). Supplemental figures and tables.

REFERENCES

1. Fuhrman JA. 1999. Marine viruses and their biogeochemical and ecological effects. Nature 399:541–548. https://doi.org/10.1038/21119
2. Hendrix RW, Smith MC, Burns RN, Ford ME, Hatfull GF. 1999. Evolutionary relationships among diverse bacteriophages and prophages: all the world's a phage. Proc Natl Acad Sci U S A 96:2192–2197. https://doi.org/10.1073/pnas.96.5.2192
3. Mushegian AR. 2020. Are there 10^{31} virus particles on earth, or more, or less? J Bacteriol 202:e00052-20. https://doi.org/10.1128/JB.00052-20
4. White RA 3rd. 2021. The future of virology is synthetic. mSystems 6:e0077021. https://doi.org/10.1128/mSystems.00770-21
5. Suttle CA. 2007. Marine viruses--major players in the global ecosystem. Nat Rev Microbiol 5:801–812. https://doi.org/10.1038/nrmicro1750
6. Bar-On YM, Phillips R, Milo R. 2018. The biomass distribution on earth. Proc Natl Acad Sci U S A 115:6506–6511. https://doi.org/10.1073/pnas.1711842115
7. Noble RT, Fuhrman JA. 1998. Use of SYBR Green I for rapid epifluorescence counts of marine viruses and bacteria. Aquat Microb Ecol 14:113–118. https://doi.org/10.3354/ame014113
8. Hobbie JE, Daley RJ, Jasper S. 1977. Use of nuclepore filters for counting bacteria by fluorescence microscopy. Appl Environ Microbiol 33:1225–1228. https://doi.org/10.1128/aem.33.5.1225-1228.1977
9. Hara S, Terauchi K, Koike I. 1991. Abundance of viruses in marine waters: assessment by epifluorescence and transmission electron microscopy. Appl Environ Microbiol 57:2731–2734. https://doi.org/10.1128/aem.57.9.2731-2734.1991
10. Wilhelm SW, Suttle CA. 1999. Viruses and nutrient cycles in the sea. BioScience 49:781–788. https://doi.org/10.2307/1313569
11. Weinbauer MG. 2004. Ecology of prokaryotic viruses. FEMS Microbiol Rev 28:127–181. https://doi.org/10.1016/j.femsre.2003.08.001

12. Rohwer F, Prangishvili D, Lindell D. 2009. Roles of viruses in the environment. Environ Microbiol 11:2771–2774. https://doi.org/10.1111/j.1462-2920.2009.02101.x
13. Jiao N, Zheng Q. 2011. The microbial carbon pump: from genes to ecosystems. Appl Environ Microbiol 77:7439–7444. https://doi.org/10.1128/AEM.05640-11
14. Breitbart M. 2012. Marine viruses: truth or dare. Ann Rev Mar Sci 4:425–448. https://doi.org/10.1146/annurev-marine-120709-142805
15. Lara E, Vaqué D, Sà EL, Boras JA, Gomes A, Borrull E, Díez-Vives C, Teira E, Pernice MC, Garcia FC, Forn I, Castillo YM, Peiró A, Salazar G, Morán XAG, Massana R, Catalá TS, Luna GM, Agustí S, Estrada M, Gasol JM, Duarte CM. 2017. Unveiling the role and life strategies of viruses from the surface to the dark ocean. Sci Adv 3:e1602565. https://doi.org/10.1126/sciadv.1602565
16. Wang S, Yang Y, Jing J. 2022. A synthesis of viral contribution to marine nitrogen cycling. Front Microbiol 13:834581. https://doi.org/10.3389/fmicb.2022.834581
17. Dupraz Christophe, Visscher PT. 2005. Microbial lithification in marine stromatolites and hypersaline mats. Trends Microbiol 13:429–438. https://doi.org/10.1016/j.tim.2005.07.008
18. Dupraz C, Reid RP, Braissant O, Decho AW, Norman RS, Visscher PT. 2009. Processes of carbonate precipitation in modern microbial mats. Earth Sci Rev 96:141–162. https://doi.org/10.1016/j.earscirev.2008.10.005
19. Dupraz C, Reid RP, Visscher PT. 2011. Microbialites, modern, p 617–635. In Reitner J, ThielV(ed), Encyclopedia of geobiology. Springer, Netherlands.
20. Burne RV, Moore LS. 1987. Microbialites: organosedimentary deposits of benthic microbial communities. Palaios 2:241. https://doi.org/10.2307/3514674
21. White III RA. 2020. The global distribution of modern microbialites: not so uncommon after all, p 107–134. In Souza V, SeguraA, FosterJS(ed), Astrobiology and cuatro ciénegas basin as an analog of early earth. Springer, Cham.
22. Nutman AP, Bennett VC, Friend CRL, Van Kranendonk MJ, Chivas AR. 2016. The rapid emergence of life was shown by the discovery of 3,700-million-year-old microbial structures. Nature 537:535–538. https://doi.org/10.1038/nature19355
23. Decho AW. 1990. Microbial exopolymer secretions in ocean environments: their role(s) in food webs and marine processes. Oceanogr Mar Biol Annu Rev 28:73–154.
24. Braissant O, Cailleau G, Dupraz C, Verrecchia EP. 2003. Bacterially induced mineralization of calcium carbonate in terrestrial environments: the role of exopolysaccharides and amino acids. J Sediment Res 73:485–490. https://doi.org/10.1306/111302730485
25. Carreira C, Staal M, Middelboe M, Brussaard CPD. 2015. Counting viruses and bacteria in photosynthetic microbial mats. Appl Environ Microbiol 81:2149–2155. https://doi.org/10.1128/AEM.02863-14
26. White RA 3rd, Visscher PT, Burns BP. 2021. Between a rock and a soft place: the role of viruses in lithification of modern microbial mats. Trends Microbiol 29:204–213. https://doi.org/10.1016/j.tim.2020.06.004
27. Marie D, Brussaard CPD, Thyrhaug R, Bratbak G, Vaulot D. 1999. Enumeration of marine viruses in culture and natural samples by flow cytometry. Appl Environ Microbiol 65:45–52. https://doi.org/10.1128/AEM.65.1.45-52.1999
28. Brussaard CPD. 2004. Optimization of procedures for counting viruses by flow cytometry. Appl Environ Microbiol 70:1506–1513. https://doi.org/10.1128/AEM.70.3.1506-1513.2004
29. Weinbauer MG, Suttle CA. 1997. Comparison of epifluorescence and transmission electron microscopy for counting viruses in natural marine waters. Aquat Microb Ecol 13:225–232. https://doi.org/10.3354/ame013225
30. Patel A, Noble RT, Steele JA, Schwalbach MS, Hewson I, Fuhrman JA. 2007. Virus and prokaryote enumeration from planktonic aquatic environments by epifluorescence microscopy with SYBR Green I. Nat Protoc 2:269–276. https://doi.org/10.1038/nprot.2007.6
31. Cunningham BR, Brum JR, Schwenck SM, Sullivan MB, John SG. 2015. An inexpensive, accurate, and precise wet-mount method for enumerating aquatic viruses. Appl Environ Microbiol 81:2995–3000. https://doi.org/10.1128/AEM.03642-14
32. Forterre P, Soler N, Krupovic M, Marguet E, Ackermann H-W. 2013. Fake virus particles generated by fluorescence microscopy. Trends Microbiol 21:1–5. https://doi.org/10.1016/j.tim.2012.10.005
33. Conceição-Neto N, Zeller M, Lefrère H, De Bruyn P, Beller L, Deboutte W, Yinda CK, Lavigne R, Maes P, Van Ranst M, Heylen E, Matthijnssens J. 2015. Modular approach to customise sample preparation procedures for viral metagenomics: a reproducible protocol for virome analysis. Sci Rep 5:16532. https://doi.org/10.1038/srep16532
34. Mikel P, Vasickova P, Kralik P. 2015. Methods for preparation of MS2 phage-like particles and their utilization as process control viruses in RT-PCR and qRT-PCR detection of RNA viruses from food matrices and clinical specimens. Food Environ Virol 7:96–111. https://doi.org/10.1007/s12560-015-9188-2
35. Pacton M, Wacey D, Corinaldesi C, Tangherlini M, Kilburn MR, Gorin GE, Danovaro R, Vasconcelos C. 2014. Viruses as new agents of organomineralization in the geological record. Nat Commun 5:4298. https://doi.org/10.1038/ncomms5298
36. Słowakiewicz M, Borkowski A, Syczewski MD, Perrota ID, Owczarek F, Sikora A, Detman A, Perri E, Tucker ME. 2021. Newly-discovered interactions between bacteriophages and the process of calcium carbonate precipitation. Geochim Cosmochim Acta 292:482–498. https://doi.org/10.1016/j.gca.2020.10.012
37. Williamson KE, Fuhrmann JJ, Wommack KE, Radosevich M. 2017. Viruses in soil ecosystems: an unknown quantity within an unexplored territory. Annu Rev Virol 4:201–219. https://doi.org/10.1146/annurev-virology-101416-041639
38. White RA 3rd, Chan AM, Gavelis GS, Leander BS, Brady AL, Slater GF, Lim DSS, Suttle CA. 2015. Metagenomic analysis suggests modern freshwater microbialites harbor a distinct core microbial community. Front Microbiol 6:1531. https://doi.org/10.3389/fmicb.2015.01531
39. White Iii RA, Wong HL, Ruvindy R, Neilan BA, Burns BP. 2018. Viral communities of Shark Bay modern stromatolites. Front Microbiol 9:1223. https://doi.org/10.3389/fmicb.2018.01223
40. Wong HL, White RA 3rd, Visscher PT, Charlesworth JC, Vázquez-Campos X, Burns BP. 2018. Disentangling the drivers of functional complexity at the metagenomic level in Shark Bay microbial mat microbiomes. ISME J 12:2619–2639. https://doi.org/10.1038/s41396-018-0208-8
41. Philippe N, Legendre M, Doutre G, Couté Y, Poirot O, Lescot M, Arslan D, Seltzer V, Bertaux L, Bruley C, Garin J, Claverie J-M, Abergel C. 2013. Pandoraviruses: amoeba viruses with genomes up to 2.5 MB reaching that of parasitic eukaryotes. Science 341:281–286. https://doi.org/10.1126/science.1239181
42. Mayor HD, Hill NO. 1961. Acridine orange staining of a single-stranded DNA bacteriophage. Virology 14:264–266. https://doi.org/10.1016/0042-6822(61)90202-1
43. Darzynkiewicz Z. 1990. Differential staining of DNA and RNA in intact cells and isolated cell nuclei with acridine orange. Methods Cell Biol 33:285–298. https://doi.org/10.1016/s0091-679x(08)60532-4
44. Saad AM, Soliman AM, Kawasaki T, Fujie M, Nariya H, Shimamoto T, Yamada T. 2019. Systemic method to isolate large bacteriophages for use in biocontrol of a wide-range of pathogenic bacteria. J Biosci Bioeng 127:73–78. https://doi.org/10.1016/j.jbiosc.2018.07.001
45. Brum JR, Hurwitz BL, Schofield O, Ducklow HW, Sullivan MB. 2016. Seasonal time bombs: dominant temperate viruses affect Southern Ocean microbial dynamics. ISME J 10:437–449. https://doi.org/10.1038/ismej.2015.125
46. Brunskill GJ, Ludlam SD. 1969. Fayetteville Green Lake,New York. I. physical and chemical limnology. Limnol Oceanogr 14:817–829. https://doi.org/10.4319/lo.1969.14.6.0817
47. Rontó G, Agamalyan MM, Drabkin GM, Feigin LA, Lvov YM. 1983. Structure of bacteriophage T7. Small-angle X-ray and neutron scattering study. Biophys J 43:309–314. https://doi.org/10.1016/S0006--3495(83)84354-9
48. Baskin RL. 2005. Calculation of area and volume for the south part of Great Salt Lake, Utah: U.S. Geological Survey Open File Report. https://doi.org/10.3133/ofr20051327